UC Irvine
UC Irvine Previously Published Works

Title

Use of polarization-sensitive optical coherence tomography to determine the directional polarization sensitivity of articular cartilage and meniscus

Permalink
https://escholarship.org/uc/item/75q1v3gf

Journal
Journal of Biomedical Optics, 11(6)

ISSN
1083-3668

Authors
Xie, Tuqiang
Guo, Shuguang
Zhang, Jun
et al.

Publication Date
2006

DOI
10.1117/1.2397574

Copyright Information
This work is made available under the terms of a Creative Commons Attribution License, available at https://creativecommons.org/licenses/by/4.0/

Peer reviewed

eScholarship.org Powered by the California Digital Library
University of California

Use of polarization-sensitive optical coherence tomography to determine the directional polarization sensitivity of articular cartilage and meniscus

Tuqiang Xie
Shuguang Guo
Jun Zhang
Zhongping Chen
George M. Peavy
University of California, Irvine
Beckman Laser Institute
Irvine, California 92612

Abstract. The directional polarization sensitivity of articular cartilage and meniscus is investigated by use of polarization-sensitive optical coherence tomography (PS-OCT) by varying the angle of incident illumination. Experimental results show that when the incident light is perpendicular to the tissue surface, normal articular cartilage demonstrates little polarization sensitivity, while meniscus demonstrates strong polarization sensitivity. Differences in optical phase retardation produced by articular cartilage and meniscus are observed when the incident angle of the scanning light beam is adjusted between 0 and 90 deg relative to the tissue surface. Directional polarization sensitivity of articular cartilage and meniscus as obtained by PS-OCT imaging using variations in the angle of incident illumination can be used to assess the orientation and organization of the collagen matrix of these tissues. The polarization sensitivity as evidenced by the Stokes vector and optical phase retardation images can be explained by the orientation of the angle of illumination relative to the unique structural organization of the collagen fibrils and fibers of articular cartilage and meniscus. © *2006 Society of Photo-Optical Instrumentation Engineers.* [DOI: 10.1117/1.2397574]

Keywords: optical coherence tomography; medical optics instrumentation; medical imaging; biological imaging; polarization-sensitive device; birefringence; polarization-sensitive optical coherence tomography; cartilage; meniscus.

Paper 05385RR received Dec. 21, 2005; revised manuscript received Jul. 31, 2006; accepted for publication Aug. 1, 2006; published online Nov. 20, 2006.

1 Introduction

Degenerative joint disease (DJD) or osteoarthritis can be a severely debilitating disease and is second only to heart disease as the most common cause of physical disability.[1] To diagnose the disease early in its onset, evaluate response to treatment, and to assist in the development of appropriate and efficacious treatment strategies, it is important to be able to accurately assess the collagen microstructure of cartilage in patients in the early stages of disease development. Diagnostic biopsy of articular cartilage is not advised because of the limited regenerative capacity of cartilage. Conventional morphological imaging methods, including radiographs, computed tomography (CT), ultrasound, and magnetic resonance imaging (MRI), have been applied to the diagnosis of cartilage abnormalities;[2–5] however, these methods provide insufficient resolution for evaluation of microstructural changes.

As a new morphological imaging technique, optical coherence tomography (OCT) allows noninvasive, high-resolution, cross sectional imaging of the tissue microstructure[6] and is adaptable to arthroscopy.[7] Conventional OCT is based on the intensity of backscattered light. Polarization-sensitive OCT (PS-OCT) provides information on the polarization states of backscattered light, revealing properties of collagen matrix organization and integrity not available by conventional OCT.[8,9] Birefringence exists in many tissues because of the presence, organization, and orientation of components such as collagen, keratin, and myelin, and the polarization properties of the tissue may be altered by injury or disease that affects the presence, organization, and/or orientation of these components. PS-OCT has been used to study the microstructure and birefringence properties of biological tissues including skin, articular cartilage, and intervertebral disk.[10–13]

Based on studies that have utilized polarized light microscopy, normal cartilage is known to demonstrate birefringence in tissue sections cut perpendicular to the articular surface and examined by transillumination.[14–16] PS-OCT has been reported to be a potentially valuable diagnostic tool for the assessment of collagen matrix changes in DJD[11,13,17,18] and reportedly can be used to differentiate osteoarthritic cartilage from normal cartilage by detecting changes in phase retardation patterns attributed to alterations in tissue birefringence. Previous experimental results were reported to demonstrate strong birefringence in healthy articular cartilage that diminishes subsequent to cartilage degeneration.[11,17,18]

Address all correspondence to Tuqiang Xie, Tel: 949 824 6837; E-mail: txie@uci.edu; Zhongping Chen, Tel: 949 824 1247; E-mail: z2chen@uci.edu; or George Peavy, Tel: 949 824 4832; E-mail: gpeavy@uci.edu; Beckman Laser Institute, 1002 Health Sciences Road East, Irvine, CA 92612; Fax: 949 824 8413.

1083-3668/2006/11(6)/064001/8/$22.00 © 2006 SPIE

Downloaded From: https://www.spiedigitallibrary.org/journals/Journal-of-Biomedical-Optics on 1/14/2019
Terms of Use: https://www.spiedigitallibrary.org/terms-of-use

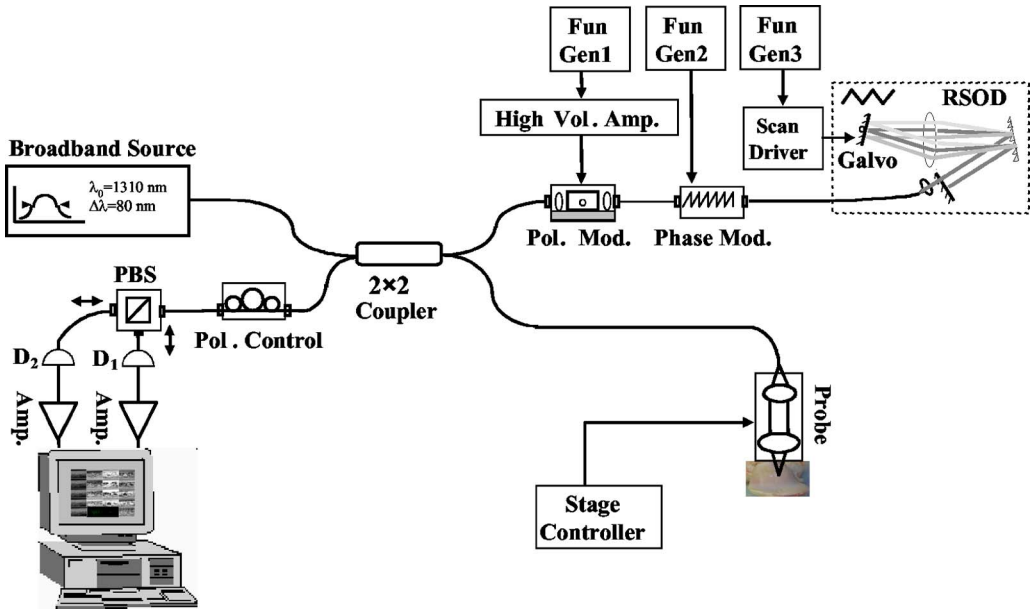

Fig. 1 Schematic diagram of PS-OCT system setup: function generator (Fun Gen); polarization modulator (Pol. Mod); polarization controllers (Pol. Control); phase modulator (Phase Mod); polarization beam splitter (PBS); rapid scanning optical delay line (RSOD); and detectors (D_1 and D_2).

Recent experimental results reported by us[13] differ from previous reports of others[11,17,18] by demonstrating that healthy articular cartilage shows little or no optical phase retardation with the optical axis normal to the articular surface. Therefore, PS-OCT cannot be used to differentiate osteoarthritic cartilage from healthy cartilage without careful consideration of the complex relationship of the sample orientation, incident angle, and polarization. In this study, the directional polarization sensitivity demonstrated by bovine articular cartilage and meniscus was evaluated by a PS-OCT system to investigate the relationship between the incident angle of illumination with respect to the collagen fiber orientation of the tissue matrix and the degree of optical phase retardation observed. Experimental results demonstrate that normal articular cartilage could appear polarization sensitive if the incident light does not scan the tissue at a normal orientation to the surface, and misinterpretation of the collagen organization or health status could happen if the angle of incident light relative to the orientation of the collagen matrix is unknown or not controlled during imaging. The directional polarization sensitivity of articular cartilage as demonstrated by our results can explain and predicate what kind of results might be observed when the scanning beam is not normal to the surface of cartilage, or the orientation of normal cartilage fibrils are not consistent throughout the whole joint.[16] This is a significant observation, as several studies (including clinical trials) are ongoing using a different interpretation of optical phase retardation in regard to tissue birefringence in assessing health and degeneration of articular cartilage.

2 Materials and Methods

The schematic diagram of the PS-OCT setup is shown in Fig. 1 and has been described previously.[13,19] Nonpolarized low coherence light from a superluminescent diode (SLD) with 10-mW output power and a central wavelength of 1310 nm with a full width at half maximum (FWHM) spectral bandwidth of 80 nm was coupled into a 2×2 fiber optic nonpolarizing coupler, which split the light into reference and sample arms. In the reference arm, a four-step driving function was applied to the polarization modulator (Newport Company, Irvine, California), and each step introduced a $\pi/4$ phase shift. Since only vertical polarized light could pass through the phase modulator, four different reference polarization states were selected and each were separated by 45-deg angles over a great circle on a Poincaré sphere. An electro-optic phase modulator (Sumitomo Osaka Cement Company Limited, Tokyo, Japan) was inserted in the reference arm and driven by a ramp waveform to generate a stable 500-kHz carrier frequency for heterodyne detection, so that the modulated interference signal could be demodulated more exactly by filtering out the low frequency noise in the system. Backscattered light from the sample was combined with the light of each of the four corresponding polarization states reflected from the reference arm. In the detector arm, the interfered beams were split into their horizontal and vertical components by a polarization beamsplitter and detected by two photodetectors (Laser Components, Incorporated, Santa Rosa, California), then high pass filtered, amplified, digitalized, and further processed by a computer.

The four corresponding polarization states scattered from the sample arm were obtained by phased-resolved processing of the interference fringe signals obtained from two perpendicular polarization detection channels. By measuring the envelope of the interferometer signal in two channels of orthogonal polarization and their phase difference, the corresponding Stokes vectors could be obtained, and the accumulative optical phase retardation was calculated as a function of depth from normalized Stokes vectors.[19,20] The four Stokes parameters I, Q, U, and V are calculated by:

Downloaded From: https://www.spiedigitallibrary.org/journals/Journal-of-Biomedical-Optics on 1/14/2019
Terms of Use: https://www.spiedigitallibrary.org/terms-of-use

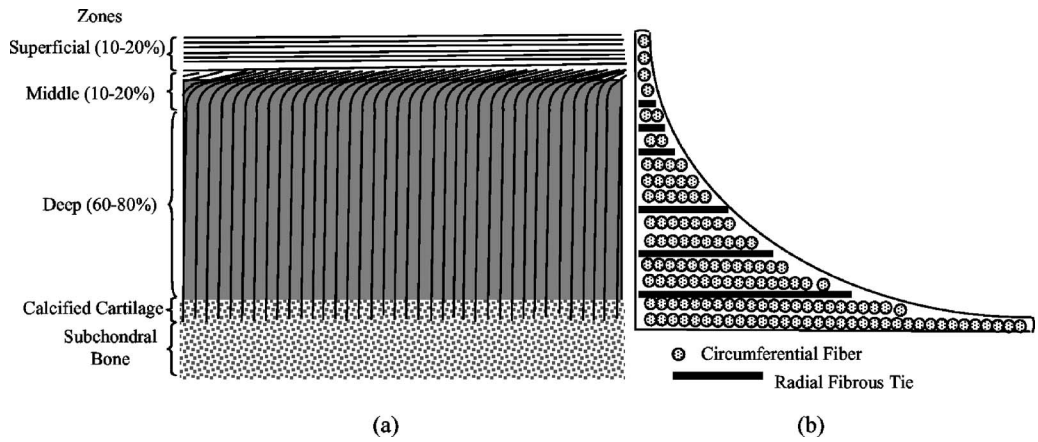

Fig. 2 Diagram of the architectural organization of the collagen matrix of (a) articular cartilage and (b) meniscus. In (a) articular cartilage, type 2 collagen fibrils extend up from the calcified cartilage zone through the deep zone in a vertical direction perpendicular to the articular surface, arch in the middle zone, and lay in a horizontal direction parallel to articular surface in the superficial zone. In (b) the meniscus, type 2 collagen fibers are grouped into bundles and fascicles that lay in a circumferential direction parallel to the periphery of the meniscus and horizontal to the articular surface.

$$I(z) = a_x^2(z) + a_y^2(z),$$

$$Q(z) = a_x^2(z) - a_y^2(z),$$

$$U(z) = 2a_x(z) \bullet a_y(z) \bullet \cos\varphi(z),$$

$$V(z) = 2a_x(z) \bullet a_y(z) \bullet \sin\varphi(z), \quad (1)$$

where a_x and a_y are amplitudes of two orthogonal components at depth z from two polarization detection channels, and φ represents the phase difference between the two components. The axial resolution (Δz) of the OCT system is determined by the coherence length of the light source and $\Delta z = (2 \ln 2/\pi) \cdot (\bar{\lambda}^2/\Delta\lambda)$, which is 10 μm in air for this system. The lateral or transverse resolution is determined by the focused spot size in analogy with conventional microscopy and is around 10 μm. The dynamic range is 60 dB, and 256 gray levels were used to display OCT images.

Articular cartilage is composed of predominantly type 2 collagen fibrils arranged in several distinct morphological zones, including the superficial zone, the middle zone, the deep zone, and the calcified zone, with different compositional and matrix organizational characteristics as illustrated in Fig. 2(a).[14–16,21–24] Meniscus is primarily composed of type 1 collagen fibers, the bulk of which are orientated parallel to each other and lay in a circumferential direction grouped into large fascicles that run parallel to the periphery of the meniscus and horizontal to the joint surface, as demonstrated in Fig. 2(b).[25] There are two major components of articular cartilage and meniscus: 1. a fluid phase containing proteoglycans and water, and 2. a solid matrix containing collagen (predominantly type 1 in meniscus and type 2 in articular cartilage). The collagen matrix contributes mostly to tensile behavior and integrity of cartilage tissue. Proteoglycans are large biomolecules that consist of a protein core with glycosaminoglycan side chains and constrained within the collagen matrix. Birefringence in cartilage is due to the asymmetrical collagen fibril structure and may change with derangement and mechanical failure of the collagen network.

Fresh bovine articular cartilage specimens were collected from the femoral-tibial joints of adult (5 to 7 years old) Holstein dairy cows slaughtered within the previous 36 h. Full thickness samples of articular cartilage that included subchondral bone were obtained for study from the articular surface of the proximal tibia by punch biopsy using a 1.0-cm-diam circular punch and mallet. A piece of meniscus was cut from whole meniscus harvested from the joint. A number 11 scalpel blade was used to make two V-shaped marks on the edge of the cartilage specimen across the center from each other, and the laser beam of the PS-OCT imaging system was scanned between these marks to obtain the specimen image. Each prepared specimen was wrapped in a 0.9% saline soaked gauze sponge, placed in a sealed and marked plastic bag, and held at room temperature until it was imaged later on the same day.

A total of eight articular cartilage and three meniscus specimens were collected and imaged. At the time of imaging, each specimen was removed from its protective wrapping, the base set in a 2×2-cm piece of paraffin for positioning and stabilization during imaging, and then placed in a 2-cm round disposable plastic petri dish. The petri dish was set on a rotation platform (PRM, Thorlabs, Newton, New Jersey) so that 3-D and angular adjustments could be made. The petri dish was positioned under the controlled motorized sample arm of the imaging system so that the scanning beam, as evidenced by illumination from a superimposed 670-nm aiming beam, could pass across the surface of the cartilage specimen between the two V-shaped marks. The incident light from the focus lens of the sample arm scans across the specimen surface in the air at a normal angle that is perpendicular (90 deg) to the surface, as shown by A in Fig. 3. In this study, the incident light beam was adjusted so that the specimen in the air was illuminated at different angles (α) (B in Fig. 3) away from the normal, and PS-OCT images were obtained with each variation of the angle of incident light. The specimens

Downloaded From: https://www.spiedigitallibrary.org/journals/Journal-of-Biomedical-Optics on 1/14/2019
Terms of Use: https://www.spiedigitallibrary.org/terms-of-use

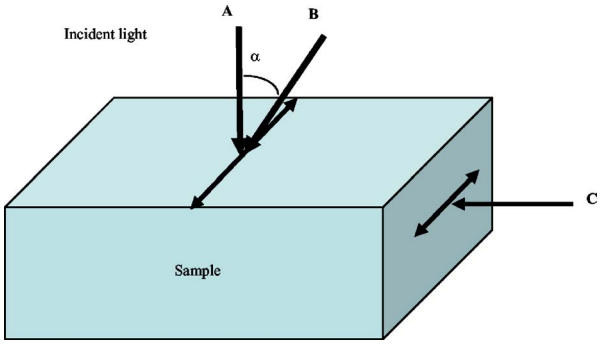

Fig. 3 Imaging directions of scanning light beam with an angle of A: 0 deg B: α, and C: 90 deg.

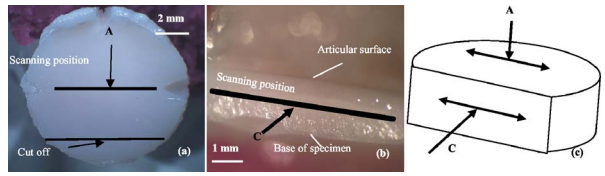

Fig. 4 Digital images of a normal articular cartilage specimen viewed through a dissecting microscope with the plane of view (a) perpendicular and (b) parallel to the specimen surface as illustrated in (c). The view (b) was made along a lateral cut surface of the specimen.

were orientated at an angle of 0 deg (normal incident), 20, 40, 60, and 75 deg from the normal direction to the specimen surface, and 90 deg where the light was incident on the vertical cut of the specimen (C in Fig. 3). Articular cartilage shows little birefringence when the incident light scans the tissue normal to the surface. In normal cartilage, the collagen fibrils are symmetrical in respect to the beam normal to the surface; therefore, the orientation of the surface collagen to the image section should be the same from any direction.

After OCT imaging, each specimen was fixed in 10% buffered formalin. Following tissue fixation, each specimen was decalcified by being placed into 8% formic acid and checked daily until soft enough to section. Samples were then dehydrated in progressive concentrations of ethanol-water, cleared with Histoclear (National Diagnostics, Manville, New Jersey), and infiltrated with paraffin in an ATP1 tissue processor (Triangle Biomedical Sciences, Durham, North Carolina). The samples were then embedded in paraffin, cut perpendicularly to the articular cartilage surface in 6-μm-thick serial sections made along the length of each specimen at its center where the OCT images had been obtained, and carefully placed on clean glass slides. The sections were deparaffinized with Histoclear, stained in hematoxylin (Sigma, Saint Louis, Missouri) and eosin-y (HE) (EM Sciences, Port Washington, Pennsylvania), and coverslipped. The histology slides were imaged using a microscope (Nikon Microphot-fxa, Tokyo, Japan) with a real-time digital color microscope imaging camera (Microfire C, Optronics, Goleta, California) coupled to a computer and recorded using image capture software (PictureFrame, ImagingPlanet, Goleta, California).

3 Results

Surface images as viewed through a dissecting microscope from the two directions are shown in Figs. 4(a) and 4(b). The OCT, Stokes vector, accumulative phase retardation, and histology images are shown in Figs. 5(a) through 5(g). The OCT image [Fig. 5(a)] correlated well with the histology [Fig. 5(g)]. In the Stokes vector images shown in Figs. 5(b) and 5(e), the vertical columns from left to right represent the four Stokes vector components, I, Q, U, and V, respectively, and the horizontal rows from top to bottom represent the four incident polarization states from the polarization modulator. It was found that normal bovine articular cartilage has little polarization sensitivity when the scanning light from the sample arm is incident on the surface of the specimen at a right angle [Figs. 5(b) and 5(c)]. In contrast, when the scanning light is incident to the deep zone of the specimen along a lateral cut surface in a direction parallel to the articular surface, the banded structure in the Stokes vector images of Fig. 5(e) clearly demonstrate that the tissue has strong polarization sensitivity, and the phase retardation image in Fig. 5(f) shows distinct retardation bands.

A plot of the phase retardation in relation to tissue depth for the two different incident directions in normal articular cartilage is shown in Fig. 6. The optical phase retardation $\delta(z)$ is determined by the relationship $\delta(z)=2\pi\Delta n\cdot z/\lambda_0$, and the degree of phase retardation $\Delta n=n_e-n_o$ can be evaluated by the slope in a graph of phase retardation $\delta(z)$ versus depth (z), since $\Delta n=(\lambda_0/2\pi)[d\delta(z)/dz]$ can be obtained from the derivation of the previous relationship, where n_e and n_o are the refractive indices for the ordinary ray and the extraordinary ray, respectively.[26,27] The graphs of phase retardation versus depth in Fig. 6 show that normal bovine articular cartilage produces little optical phase retardation when the direction of incident illumination is perpendicular to the articular surface but strong phase retardation is observed when the incident direction is parallel to the articular surface and perpendicular

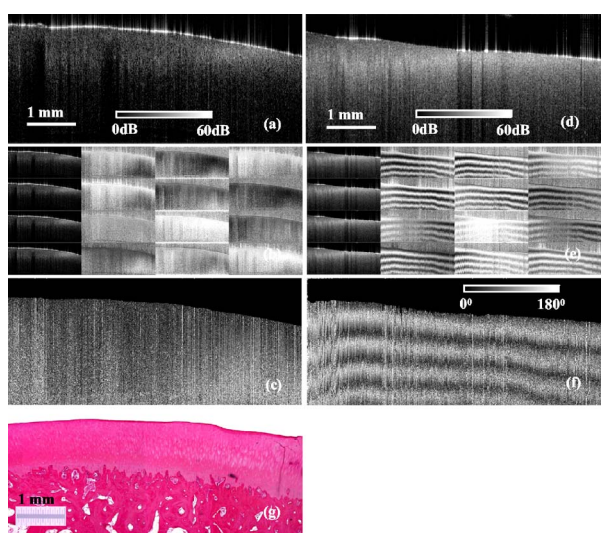

Fig. 5 (a) and (d) OCT images and (b) and (e) Stokes vector images (6×2.8 mm) and (c) and (f) phase retardation images and (g) histology when the incident light scanned a normal bovine articular cartilage specimen from (a), (b), and (c) the perpendicular to the articular surface and (d), (e), and (f) and along a cut plane made 90 deg to the articular surface.

Downloaded From: https://www.spiedigitallibrary.org/journals/Journal-of-Biomedical-Optics on 1/14/2019
Terms of Use: https://www.spiedigitallibrary.org/terms-of-use

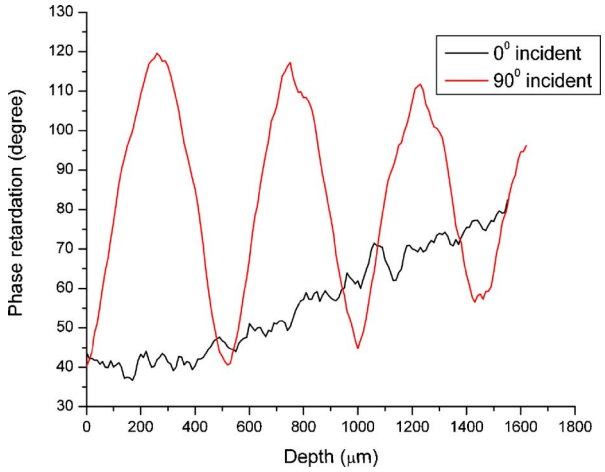

Fig. 6 Phase retardation versus depth when the incident light scanned a normal bovine articular cartilage specimen in perpendicular (0 deg) and parallel (90 deg) directions relative to the specimen surface.

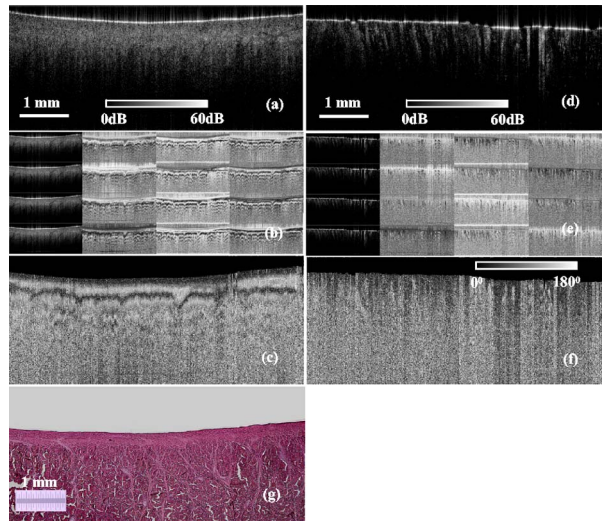

Fig. 8 (a) and (d) OCT images and (b) and (e) Stokes vector images (6×2.8 mm), (c) and (f) phase retardation images and (g) histology when the incident light scanned a normal bovine meniscus specimen (a), (b), and (c) perpendicular and (d), (e), and (f) along a cut plane made 90 deg to the surface.

to the orientation of collagen fibrils of the deep zone. Additionally, the ideal phase retardation should reach 0 and 180 deg, while experimentally it cannot because of the OCT background noise. For phase retardation close to 0 or 180 deg, the background noise introduces a significant and systematic error. This phenomenon has been reported by several groups.[20,26,27] Averaging of 20 pixels at the same depth here is used to reduce the fluctuations in phase calculation due to noise.

A specimen sectioned from a bovine meniscus is shown in Fig. 7 and was imaged by the PS-OCT system with the incident directions being perpendicular and parallel to the specimen surface. The OCT, Stokes vector, accumulative phase retardation, and histology images are shown in Figs. 8(a) through 8(g). The Stokes vector images and phase retardation images clearly demonstrate that the meniscus has strong polarization sensitivity when the incident scanning beam is normal to the meniscus surface, but little polarization sensitivity is observed when the incident beam is directed along the cut surface. The graphs of accumulative phase retardation versus depth are shown in Fig. 9 and illustrate that the meniscus produces strong phase retardation in the normalized incident direction and little phase retardation when the incident beam is aimed in a direction parallel to the meniscus surface and scanned along the vertical cut.

To further investigate the directional polarization sensitivity of the two kinds of tissues, PS-OCT images were obtained using different scanning angles relative to the articular and meniscus surfaces. The Stokes vector and phase retardation images of normal articular cartilage are shown in Figs. 10(a) through 10(j) when the incident light beam is 0, 20, 40, 60, and 75 deg from the normal to the tissue surface. The images demonstrate that the tissue produces little optical phase retardation when the incident light beam scans the tissue at the

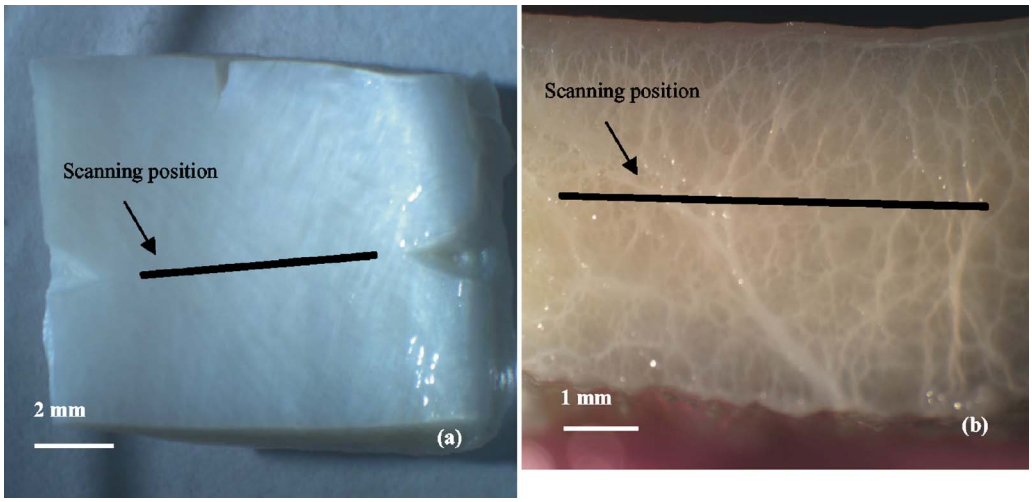

Fig. 7 Digital images of a normal bovine meniscus specimen viewed through a dissecting microscope from (a) the perpendicular and (b) parallel directions relative to the specimen surface. The view (b) was made along a vertical cut surface of the specimen.

Downloaded From: https://www.spiedigitallibrary.org/journals/Journal-of-Biomedical-Optics on 1/14/2019
Terms of Use: https://www.spiedigitallibrary.org/terms-of-use

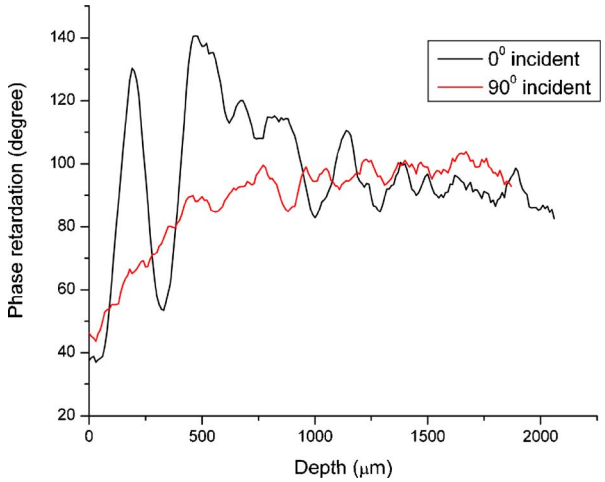

Fig. 9 Phase retardation versus depth when the incident light scanned a specimen of normal bovine meniscus from the perpendicular (0 deg) and parallel (90 deg) directions relative to the specimen surface.

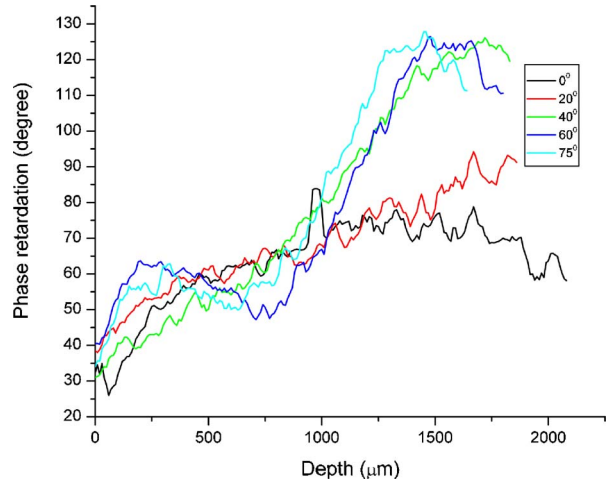

Fig. 11 Plot of phase retardation versus depth in normal bovine articular cartilage when the incident light beam is 0, 20, 40, 60, and 75 deg from the perpendicular to the articular surface.

normal (0-deg) direction to the surface, but the degree of polarization sensitivity increases when the incident angle increases from the normal. The graphs of the phase retardation versus the depth for different incident angles of normal articular cartilage are shown in Fig. 11. The phase retardation curve was calculated by averaging 20 adjacent pixels at each depth from a region where there was no intensity saturation.

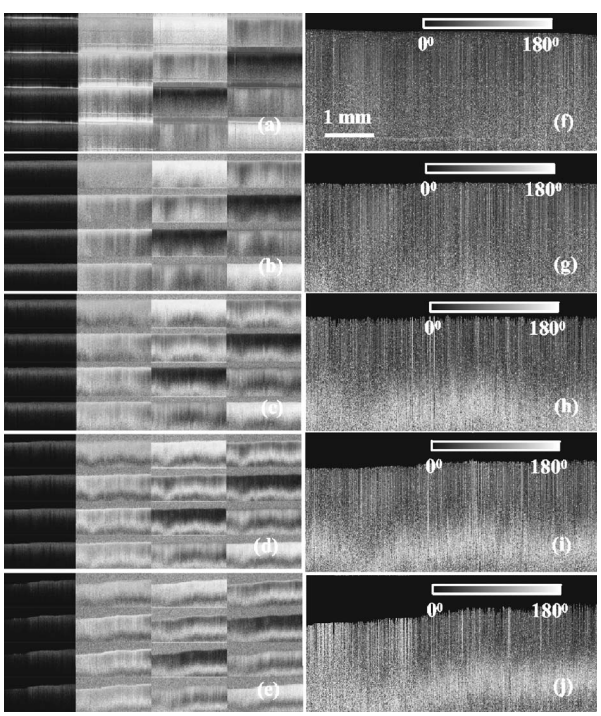

Fig. 10 (a) through (d) Stokes vector images (6×2.8 mm) and (f) through (j) phase retardation images of a normal articular cartilage when the incident light beam is (a) and (f) 0 deg (b) and (g) 20 deg, (c) and (h) 40 deg, (d) and (i) 60 deg, and (e) and (j) 75 deg from the perpendicular to the articular surface.

The Stokes vector images in Figs. 12(a) through 12(e) and the phase retardation images in Figs. 12(f) through 12(j) of a normal bovine meniscus specimen were obtained with the incident light beam 0 deg [12(a) and 12(f)], 20 deg [12(b) and 12(g)], 40 deg [12(c) and 12(h)], 60 deg [12(d) and 12(i)], and 70 deg [12(e) and 12(j)] from the normal to the specimen surface. The banded structure in the Stokes vector and phase retardation images demonstrates the polarization sensitivity of the specimen, and shows that the degree of phase retardation produced by the tissue decreases with the increasing incident angle away from the normal. The graphs in Fig. 13 demon-

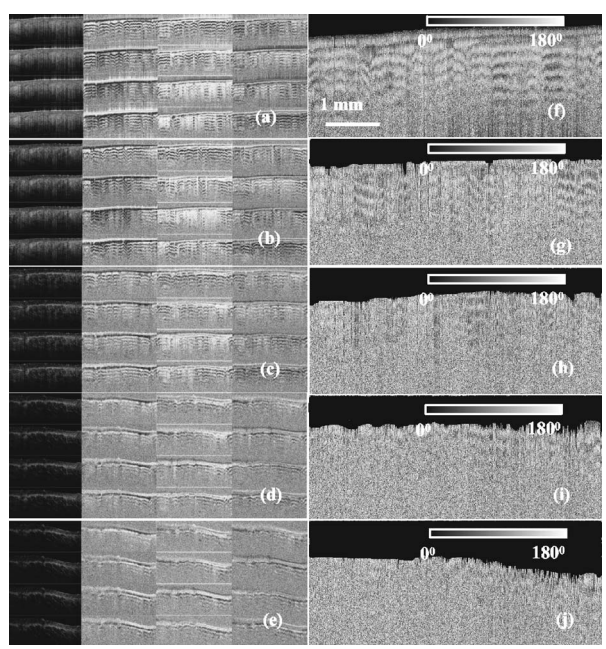

Fig. 12 (a) through (e) Stokes vector images (6×2.8 mm) and (f) through (j) phase retardation images of a bovine meniscus specimen made with the incident light beam (a) and (f) 0 deg, (b) and (g) 20 deg, (c) and (h) 40 deg, (d) and (i) 60 deg, and (e) and (j) 70 deg from the perpendicular to the meniscus surface.

Downloaded From: https://www.spiedigitallibrary.org/journals/Journal-of-Biomedical-Optics on 1/14/2019
Terms of Use: https://www.spiedigitallibrary.org/terms-of-use

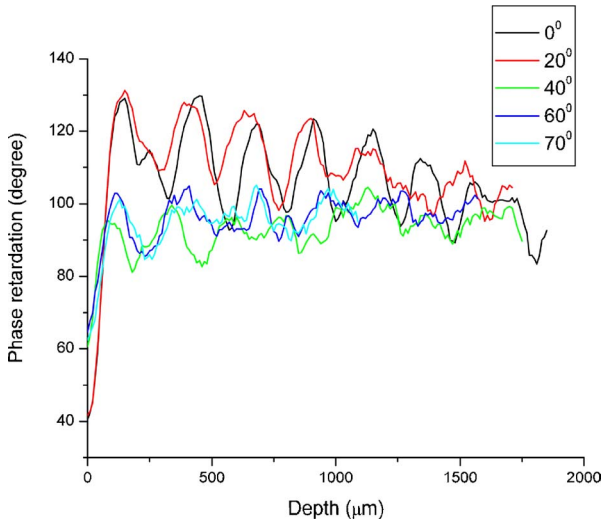

Fig. 13 Plot of phase retardation versus depth from a bovine meniscus specimen when the incident light beam is 0, 20, 40, 60, and 70 deg from the perpendicular to the meniscus surface.

strate that the phase retardation of the meniscus is strongest when the incident light scans the tissue in the normal (perpendicular) direction to the surface, and the degree of phase retardation decreases as the incident angle is increased away from the normal.

4 Discussion and Conclusions

The degree of birefringence of articular cartilage is related to the orientation and organization of the collagen fibrillar network of the cartilage matrix.[14–16] In the superficial zone of articular cartilage, the collagen fibrils are oriented parallel to the surface; therefore, the phase retardation of a beam directed normal to the articular surface is expected to increase with depth in this region. The effect on phase retardation in the superficial zone may be reduced from what might be anticipated, however, as the individual collagen fibrils lay in layered planes parallel to the surface that vary in orientation at angles of up to 45 deg to each other.[28] Minimal birefringence is expected in the middle zone, which lacks coherent orientation of the fibrils.[14–16] As the incident beam travels into the deep zone, it is traveling parallel to the orientation of the collagen fibrils in this region, and minimal to no phase retardation is expected. Consistent with this prediction, normal articular cartilage was found to produce little phase retardation when the imaging beam was directed at normal incidence to the cartilage surface. This observation is contrary to the results of previous reports that used a single detector OCT imaging system without quantification of phase retardation[11,17,18] but are consistent with results reported by another group that used a two-detector two-polarization-state PS-OCT system to study equine articular cartilage.[29]

The optical axis of collagen parallels the orientation of collagen fibrils, and maximum polarization sensitivity appears when the orientation of the incident light beam is perpendicular to the collagen fibrils. PS-OCT imaging of articular cartilage obtained with the incident beam normal to the cut surface demonstrates phase retardation along the same optical axis, as is typically reported for polarized light microscopy studies of articular cartilage.[14–16] As anticipated, the deep zone in this study demonstrated strong polarization sensitivity when the incident light was directed along a cut surface, perpendicular to the orientation of the collagen fibrils.

This study demonstrates that the amount of phase retardation evidenced by PS-OCT imaging of articular cartilage and fibrocartilage is dependent on the angle of incidence of the scanning beam relative to the orientation of the collagen fibrils in the specimen. The results reported here for articular cartilage are consistent with another PS-OCT study of articular cartilage,[29] and do not support the conclusions of others that normal, healthy cartilage can be expected to show strong birefringence as evidenced by banding in OCT images. Clearly, articular cartilage that demonstrates strong optical phase retardation by PS-OCT imaging when the incident beam is directed across a vertical cut surface can also demonstrate very little phase retardation when the beam is directed normal to the articular surface. Additionally, it is known that the orientation of collagen fibrils in relation to the joint surface can vary between locations within a joint, especially when approaching the edges of a joint;[15,16] therefore, normal differences in collagen matrix orientation relative to an imaging beam directed normal to the articular surface are likely to give substantially different pictures of phase retardation that would be inappropriate to attribute to degenerative alterations in the birefringence properties of the tissue.

The orientation of collagen fibers in the meniscus is different from that observed for articular cartilage. Collagen fibrils of the meniscus are organized into fiber bundles that run parallel to the surface.[25,30] The meniscus demonstrates strong polarization sensitivity when the incident light scan is made perpendicular to the surface, but does not demonstrate polarization sensitivity when scanning with the incident light in a direction parallel to the orientation of the collagen fibers. The experimental results demonstrate that the degree of polarization sensitivity of normal articular cartilage increases as the angle of the incident light increases away from the perpendicular to the tissue surface, but the degree of polarization sensitivity observed for meniscus decreases with an increase in the angle of incident illumination away from the perpendicular. This directional sensitivity is related to the angle of incidence of the scanning beam relative to the orientation of the collagen fibrils and fibers of the cartilage matrix, and needs to be considered when interpreting measurements of phase retardation of cartilage to assess health and disease.

In summary, PS-OCT images obtained from a two-detector PS-OCT system that uses four polarization states of light to construct Stokes vector and depth resolved accumulative phase retardation images can be used to evaluate the orientation of the collagen matrix of articular cartilage and meniscus. Images obtained from this system with the incident beam scanning perpendicular to the joint surface show that normal articular cartilage may demonstrate only mild polarization sensitivity, but that the meniscus shows strong polarization sensitivity. The degree of polarization sensitivity of both normal articular cartilage and meniscus changes when the light incident angle changes from 0 to 90 deg. These directional changes in optical phase retardation are related to the incident angle of illumination relative to the orientation of collagen fibrils and fibers of the cartilage matrix, and may be able to

Downloaded From: https://www.spiedigitallibrary.org/journals/Journal-of-Biomedical-Optics on 1/14/2019
Terms of Use: https://www.spiedigitallibrary.org/terms-of-use

provide valuable information regarding the tissue matrix in healthy and diseased states. Additionally, this information underscores the importance of recognizing that variations in the incident angle may provide differences in images obtained from the same specimen, or from different areas of a joint where variations of surface contour or matrix organization may present different orientations of the collagen matrix to an arthroscopic imaging probe.

Acknowledgments

We are pleased to acknowledge the assistance of Lih-huei Liaw, Paula Sweet, and Sharon Evander in the acquisition of specimens and histological processing. This work was supported by the U.S. Air Force Office of Scientific Research, Medical Free-Electron Laser Program (F49620-00-1-0371), the National Center for Research Resources of the National Institutes of Health (Laser Microbeam and Medical Program, RR-01192), the National Cancer Institute (CA-91717), and the Arnold and Mabel Beckman Foundation. The U.S. government is authorized to reproduce and distribute reprints for governmental purposes notwithstanding any copyright notation. The views and conclusions contained herein are those of the authors and should not be interpreted as necessarily representing the official policies or endorsements, either expressed or implied, of the Air Force Research Laboratory or the U.S. Government.

References

1. "Osteoarthritis," U.S. National Institute of Health, National institute of Arthritis and Musculoskeletal and Skin Diseases (2002).
2. D. L. Batiste, A. Kirkley, S. Laverty, L. M. Thain, A. R. Spouge, and D. W. Holdsworth, "Ex vivo characterization of articular cartilage and bone lesions in a rabbit ACL transection model of osteoarthritis using MRI and micro-CT," *Osteoarthritis Cartilage* **12**(12), 986–996 (2004).
3. M. Recht, V. Bobic, D. Burstein, D. Disler, G. Gold, M. Gray, J. Kramer, P. Lang, T. McCauley, and C. Winalski, "Magnetic resonance imaging of articular cartilage," *Clin. Orthop. Relat. Res.* **391**(suppl.), s379–s396 (2001).
4. F. Eckstein and C. Glaser, "Measuring cartilage morphology with quantitative magnetic resonance imaging," Semin. Musculoskelet. Radiol. **8**(4), 329–353 (2004).
5. H. J. Nieminen, J. Töyräs, J. Rieppo, M. T. Nieminen, J. Hirvonen, R. Korhonen, and J. S. Jurvelin, "Real-time ultrasound analysis of articular cartilage degradation *in vitro*," *Ultrasound Med. Biol.* **28**, 519–525 (2002).
6. A. D. Aguirre, P. Hsiung, T. H. Ko, I. Hartl, and J. G. Fujimoto, "High-resolution optical coherence microscopy for high-speed, in vivo cellular imaging," *Opt. Lett.* **28**, 2064–2066 (2003).
7. Y. Pan, Z. Li, T. Xie, and C. R. Chu, "Hand-held arthroscopic optical coherence tomography for in-vivo high-resolution imaging of articular cartilage," *J. Biomed. Opt.* **8**(4), 648–654 (2003).
8. J. F. de Boer, T. E. Milner, M. J. C. van Gemert, and J. S. Nelson, "Two-dimensional birefringence imaging in biological tissue by polarization-sensitive optical coherence tomography," *Opt. Lett.* **22**, 934–936 (1997).
9. S. Jiao and L. Wang, "Jones Matrix imaging of biological tissues with quadruple-channel optical coherence tomography," *J. Biomed. Opt.* **7**(3), 350–358 (2002).
10. C. E. Saxer, J. F. De Boer, B. H. Park, Y. Zhao, Z. Chen, and J. S. Nelson, "High-speed fiber-based polarization-sensitive optical coherence tomography of in vivo human skin," *Opt. Lett.* **25**, 1355–1357 (2000).
11. W. Drexler, D. Stamper, C. Jesser, X. Li, C. Pitris, K. Saunders, S. Martin, M. B. Lodge, J. G. Fujimoto, and M. E. Brezinski, "Correlation of collagen organization with polarization sensitive imaging of in vitro cartilage: implications for osteoarthritis," *J. Rheumatol.* **28**, 1311–1318 (2001).
12. S. J. Matcher, C. P. Winlove, and S. V. Gangnus, "The collagen structure of bovine intervertebral disc studied using polarization-sensitive optical coherence tomography," *Phys. Med. Biol.* **49**, 1295–1306 (2004).
13. T. Xie, S. Guo, J. Zhang, Z. Chen, and G. M. Peavy, "Determination of characteristics of degenerative joint disease using optical coherence tomography and polarization sensitive optical coherence tomography," *Lasers Surg. Med.* **38**, 852–865 (2006).
14. J. P. A. Arokoski, M. M. Hyttinen, T. Lapveteläinen, P. Takács, B. Kosztáczky, L. Mödis, V. Kovanen, and K. Helminen, "Decreased birefringence of the superficial zone collagen network in the canine knee (stifle) articular cartilage after long distance running training, detected by quantitative polarized light microscopy," *Ann. Rheum. Dis.* **55**, 253–264 (1996).
15. Y. Xia, J. B. Moody, H. A. Alhadlaq, N. Burton-Wurstert, and G. Lust, "Characteristics of topographical heterogeneity of articular cartilage over the joint surface of a humeral head," *Osteoarthritis Cartilage* **10**, 370–380 (2002).
16. Y. Xia, J. B. Moody, H. Alhadlaq, and J. Hu, "Imaging the physical and morphological properties of a multi-zone young articular cartilage at microscopic resolution," *J. Magn. Reson Imaging* **17**, 365–374 (2003).
17. J. M. Herman, C. Pitris, B. E. Bouma, S. A. Boppart, C. A. Jesser, D. L. Stamper, J. G. Fujimoto, and M. E. Brezinski, "High resolution imaging of normal and osteoarthritic cartilage with optical coherence tomography," *J. Rheumatol.* **26**, 627–635 (1999).
18. X. Li, S. Martin, C. Pitris, R. Ghanta, D. Stamper, M. Harman, J. G. Fujimoto, and M. E. Brezinski, "High-resolution optical coherence tomographic imaging of osteoarthritic cartilage during open knee surgery," *Arthritis Res. Ther.* **7**, R318–R323 (2005).
19. J. Zhang, S. Guo, W. Jung, J. S. Nelson, and Z. Chen, "Determination of birefringence and absolute optic axis orientation using polarization-sensitive optical coherence tomography with PM fibers," *Opt. Express* **11**, 3262–3270 (2003).
20. B. H. Park, C. Saxer, S. M. Sringivas, J. S. Nelson, and J. F. de Boer, "In vivo burn depth determination by high-speed fiber-based polarization sensitive optical coherence tomography," *J. Biomed. Opt.* **6**, 474–479 (2002).
21. M. A. MacConiall, "The movements of bones and joints: 4. the mechanical structure of articulating cartilage," *J. Bone Jt. Surg., Br. Vol.* **33B**, 251–257 (1951).
22. C. Weiss, L. Rosenberg, and A. J. Helfet, "An ultrastructural study of normal young adult human articular cartilage," *J. Bone Jt. Surg., Am. Vol.* **50**, 663–674 (1968).
23. J. M. Clark, "The organization of collagen in cryofractured rabbit articular cartilage: a scanning electron microscopic study," *J. Orthop. Res.* **3**, 17–29 (1985).
24. J. Dunham, D. R. Shackleton, M. E. J. Billingham, L. Bitensky, J. Chayen, and H. Muir, "A reappraisal of the structure of normal canine articular cartilage," *J. Anat.* **157**, 89–99 (1988).
25. S. L. Y. Woo, K. N. An, S. P. Arnoczky, J. S. Wayne, D. C. Fithian, and B. S. Meyers, "Anatomy biology and biomechanics of tendon, ligament and meniscus," in *Orthopaedic Basic Science*, S. R. Simon, Ed., pp. 45–87, American Academy of Orthopaedic Surgeons (1994).
26. J. F. de Boer and T. E. Milner, "Review of polarization sensitive optical coherence tomography and Stokes vector determination," *J. Biomed. Opt.* **7**(3), 359–371 (2002).
27. S. M. Srinivas, J. F. de Boer, H. Park, K. Keikhanzadeh, H. L. Huang, J. Zhang, W. Q. Jung, Z. Chen, and J. S. Nelson, "Determination of burn depth by polarization-sensitive optical coherence tomography," *J. Biomed. Opt.* **9**(1), 207–212 (2004).
28. J. M. Clark, "The organization of collagen fibrils in the superficial zones of articular cartilage," *J. Anat.* **171**, 117–130 (1990).
29. N. Ugryumova, D. P. Attenburrow, C. P. Winlove, and S. J. Matcher, "The collagen structure of equine articular cartilage, characterized using polarization-sensitive optical coherence tomography," *J. Phys. D* **38**, 2612–2619 (2005).
30. O. Hauger, L. R. Frank, R. D. Boutin, N. Lektrakul, C. B. Chung, P. Haghighi, and D. Resnick, "Characterization of the 'red zone' of knee meniscus: MR imaging and histologic correlation," *Radiology* **217**, 193–200 (2000).

Downloaded From: https://www.spiedigitallibrary.org/journals/Journal-of-Biomedical-Optics on 1/14/2019
Terms of Use: https://www.spiedigitallibrary.org/terms-of-use